Fröck *et al. Advanced Modeling and Simulation in Engineering Sciences(2023)10:8*
https://doi.org/10.1186/s40323-023-00247-x

Advanced Modeling and Simulation in Engineering Sciences

RESEARCH ARTICLE Open Access

Numerical modelling of the process chain for aluminium Tailored Heat-Treated Profiles

Hannes Fröck[1*], Matthias Graser[2], Michael Reich[1], Michael Lechner[2], Marion Merklein[2] and Olaf Kessler[1,3]

*Correspondence: hannes.froeck@uni-rostock.de
[1]Faculty of Mechanical Engineering and Marine Technology, Chair of Materials Science, University of Rostock, Albert-Einstein-Straße 2, 18059 Rostock, Germany
[2]Institute of Manufacturing Technology, Friedrich-Alexander-Universität Erlangen-Nürnberg, Egerlandstraße 11-13, 91058 Erlangen, Germany
[3]Department Life, Light &Matter (Research competence centre CALOR), Faculty of Interdisciplinary Research, University of Rostock, Albert-Einstein-Str. 25, 18059 Rostock, Germany

Abstract

Lightweight construction in modern car design leads to an increased usage of various aluminium semi-finished products. Besides sheet material, aluminium extrusion profiles are frequently used due to their high stiffness and variety of possible cross-sections. However, similar to sheet material, aluminium profiles exhibit limited formability in comparison to mild steel materials. One possibility to increase the forming limits of precipitation hardened aluminium alloys is the so-called Tailored Heat Treatment technology. By a local short-term heat treatment, the material is softened and the material flow can be controlled to reduce stresses in critical forming zones. The purposeful definition of the heat treatment zones is mandatory to improve the forming results. Therefore, numerical methods are necessary. In this investigation, a numerical process chain is presented. It combines the thermo-mechanical simulation of a local laser heat treatment with a subsequent bending process of the heat-treated profile using the alloy EN AW-6082. The temperature distribution, mechanical properties, and finally, the bending result of the numerical model are validated by experimental tests.

Keywords: Aluminium alloy, EN AW-6082, Tailored Heat-Treated Profiles, Process chain simulation, Material model, Bending simulation, Anisotropy, LS-Dyna

Introduction

Recently, the usage of aluminium alloys has steadily increased due to the rising importance of lightweight construction due to the concerns of emission reduction [1]. However, parts made of mild steels can often not be substituted by aluminium parts because of their comparatively low formability. One approach to increase the formability of aluminium sheet material is the use of so-called Tailored Heat-Treated Blanks (THTB). By a local short-term heat treatment, the precipitates are dissolved in the aluminium matrix such that less obstacles hinder the dislocation movement, and the material is locally softened. By the interaction of soft and hard zones, the material flow can be modified to reduce stresses in critical forming zones [2].

For a purposeful design of the heat treatment layouts, numerical analysis is needed to predict the material's behaviour, identify critical areas on the part, and design the heat-treated zones accordingly. One of the early investigations regarding the use of heat treatment layouts for increasing the formability of precipitation hardened aluminium alloys was conducted by [3], who characterised the material softening of AlMg0.4Si1.2 by laser heat treatment. In addition, the influence of the heat treatment on the formability of deep drawn cups was analysed and compared to analytically calculated data. They showed an increase of the deep drawing limits as well as a good correspondence between the analytical and experimental results. Especially in the last few years, based on the fast development in the field of FE-simulation and increasing computing capacities, various numerical approaches to improve the design of the heat treatment layouts have been developed. One example for this is an inverse approach presented by [4] who used the results of the forming simulation to derive and optimise a suitable heat treatment layout. However, a precise characterisation of the mechanical properties and modelling of the material behaviour is mandatory for a realistic calculation of the heat treatment and forming processes. In this context, [5] presented the material modelling of the aluminium blank material AA6014 PX regarding the hardening, yielding, anisotropy, as well as the failure behaviour. Based on an extensive material characterisation and considering the maximum heat treatment temperature, as well as the natural ageing duration, heat treatment layouts were derived for the enhancement of the formability of deep drawing parts in the automotive industry. In most investigations, the material behaviour in simulations is modelled according to the maximum temperatures during heat treatment based on an experimental or numerical analysis. Therefore, the influence of heating and cooling rates, as well as residual stresses due to temperature gradient effects, are neglected. In addition, in the case of many semi-finished aluminium products (e.g. rolled blanks, extrusion profiles) a high anisotropic behaviour of the material is present [6], which influences material thinning as well as geometrical deformations during bending processes [7]. Thus, the aim of this investigation is the transfer of the THTB approach on Aluminium Tailored Heat-Treated Profiles (THTP), and the development of a numerical model of the THTP process chain. Especially, heat treatment simulation results (microstructures, properties, residual stresses, deformations) should be transferred to the forming simulation. As an application example, a numerical process chain consisting of a thermo-mechanical simulation of a short-term laser heat treatment will be combined with a subsequent tube bending simulation of an aluminium extrusion profile (Fig. 1). The numerical data will be compared with experimental results regarding temperature distribution, the resulting mechanical properties, and the use of optical strain measurement.

Former investigations of the application of Tailored Heat Treatment mainly focused on improving deep drawing processes of blanks in the automotive field. However, due to the increased use of high strength alloys and higher design demands, new challenges have also arisen regarding the bending of aluminium extrusion profiles. During the tube bending process of aluminium hollow extrusion profiles, the appearance of different failure types is documented. The reason for this is the typical bending moment induced stress distribution over the profile cross-section (Fig. 2).

Cross-section deformations appear for parts with high bending angles and small curvatures. Radial forces on the flanges of the profile lead to a lateral bulging of the profile walls, and the compressive stresses on the inner radius promote the formation of wrinkles

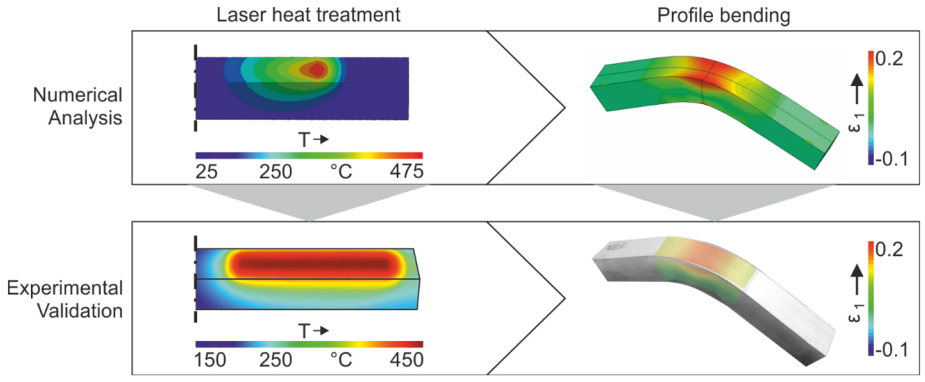

Fig. 1 High level overview of numerical process chain and the respective experimental testing

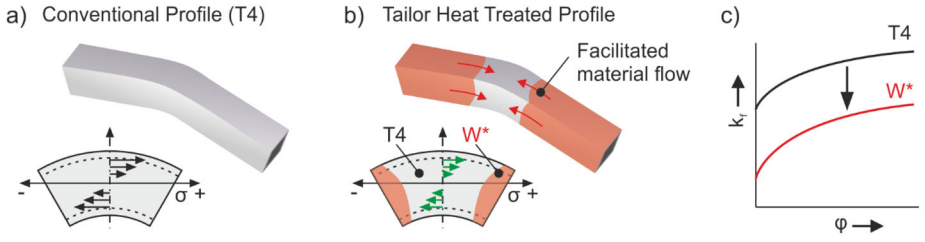

Fig. 2 Material flow mechanism of THTP

Table 1 Mass fraction of the alloying elements in the investigated alloy

Alloy	Mass fraction in %							
	Si	Fe	Cu	Mn	Mg	Cr	Zn	Al
OES EN AW-6082 T4	0.94	0.19	0.05	0.58	0.76	0.08	0.20	Balance
DIN EN 573-3 (6082)	0.7–1.3	≤ 0.5	≤ 0.1	0.4–1.0	0.6–1.2	≤ 0.25	≤ 0.25	Balance

and may result in the collapse of the cross-section. An excessive material thinning on the outer radius can be observed due to high tensile stresses (Fig. 2a), which finally leads to necking failure and an increasing rate of defective parts. By local short-term heat treatments on the distinctive profile sides, the material is softened (Fig. 2c) and the material flow is facilitated. Thus, the critical failure tensile and compressive stresses in the forming zone can be reduced (Fig. 2b) so giving the possibility to improve the bending result with respect to the maximum achievable bending angle, as well as the geometrical aspects.

Short-term heat treatment simulation

The simulation model was implemented using the finite element software LSDyna, which is suitable for heat treatment simulation as well as for bending simulation. Using the same software is very beneficial for transferring outputs of the heat treatment simulation as inputs for the subsequent bending simulation.

The material model was adapted to the precipitation hardening aluminium alloy EN AW6082 in the natural aged state (T4). A hollow quadratic extrusion profile 40 mm × 40 mm × 3 mm was used. The chemical composition of the investigated alloy is given in Table 1.

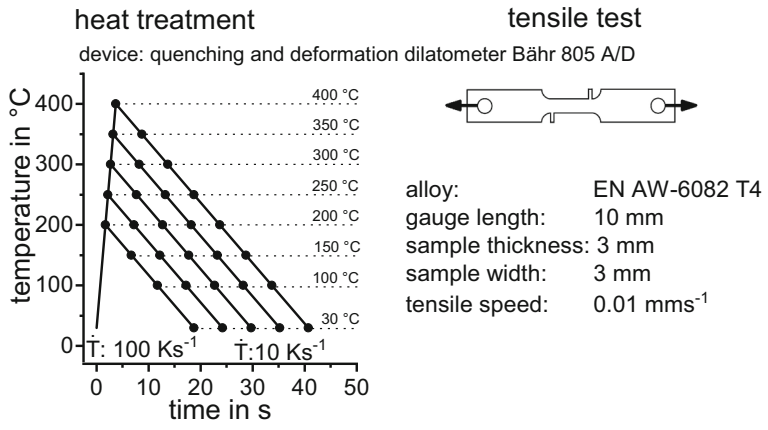

Fig. 3 Schematic time-temperature profile and essential parameters of the thermo-mechanical analysis to record load-elongation diagrams during a heat treatment with the heating rate of 100 Ks^{-1} to different maximum temperatures, and subsequent cooling at 10 Ks^{-1}

Mechanical material model

The strength of precipitation-hardening aluminium alloys, such as EN AW6082, is achieved by finely dispersed particles in the aluminium matrix. The precipitation state of an aluminium alloy therefore has a significant influence on the mechanical properties. A continuous time-temperature-dissolution diagram has already been established for the alloy under investigation, which was recorded by means of thermal analysis by differential scanning calorimetry (DSC) [8]. This diagram is the basis for the following developed mechanical material model. In order to correlate the findings from the thermal analysis with the mechanical properties, tensile tests were carried out in a quenching and deformation dilatometer type BÄHR 805 A/D (BÄHR Thermoanalyse GmbH). The experimental details for recording force-extension curves in the device used can be found in [9]. For this purpose, tensile tests were performed during heating, as well as during cooling, after different maximum temperatures at different actual temperatures. A laser short-term heat treatment is characterised by a very high heating rate of a few 100 Ks^{-1} and a subsequent rapid cooling with a few 10 Ks^{-1} [10]. In order to reproduce the temperature profile during a short-term heat treatment, a constant heating rate of 100 Ks^{-1} and a cooling rate of 10 Ks^{-1} were used for the thermo-mechanical analysis. The schematic time-temperature profile, as well as the essential parameters of the thermo-mechanical analysis during the short-term heat treatment, are shown in Fig. 3 on the left. In addition, tensile tests were carried out to room temperature after different maximum temperatures of a short-term heat treatment, as shown in Fig. 3 on the right.

The used quenching and deformation dilatometer require a customised tensile specimen geometry (see Fig. 3). This tensile specimen geometry was specially developed for the device [9], but deviates from the standard tensile specimen geometry. However, it could be shown that the results are comparable to those of standard tensile specimens [11].

Figure 4 displays the yield and tensile strengths of the alloy EN AW6082 T4 during heat treatments to different maximum temperatures during heating at 100 Ks^{-1} and cooling at 10 Ks^{-1}. Figure 4a shows that the yield and the tensile strength decrease continuously during heating up to 200 °C. During the subsequent cooling, the strength increases again. However, the initial strength is not completely recovered. A slight softening can

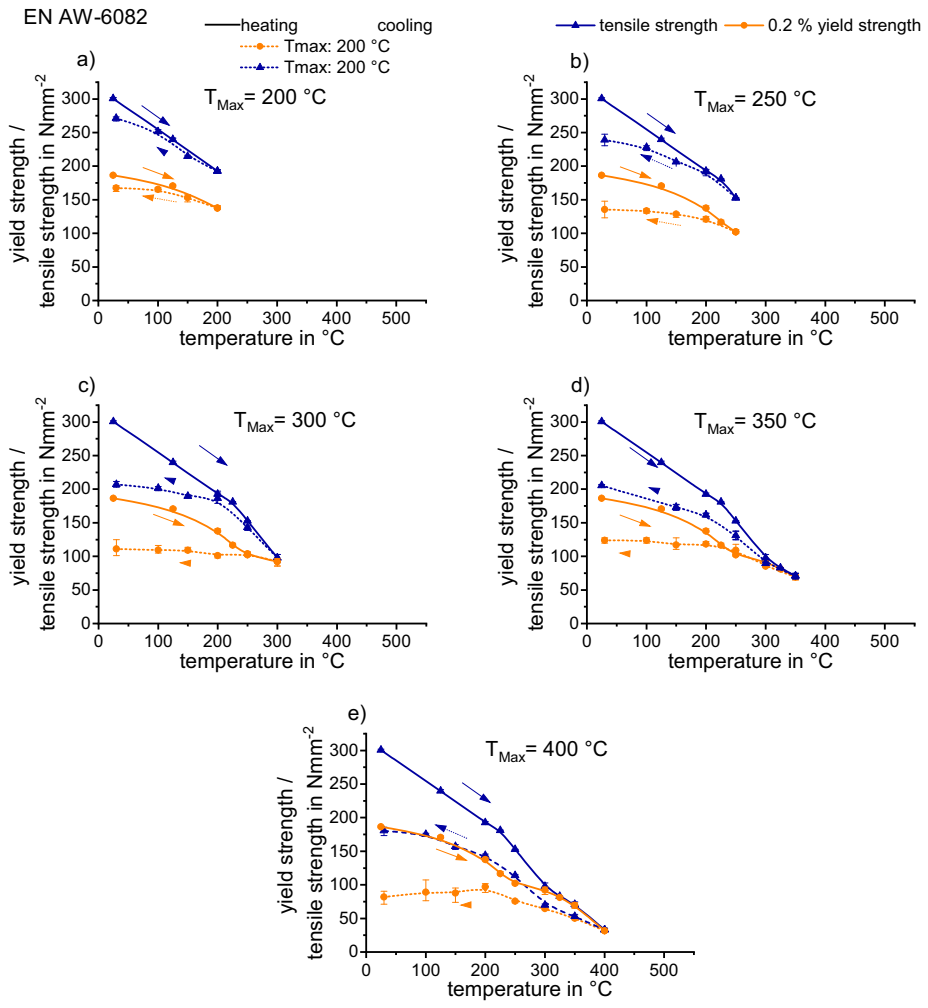

Fig. 4 Yield and tensile strength of the alloy EN AW6082 T4 during heat treatments to different maximum temperatures during heating at 100 Ks^{-1} and cooling at 10 Ks^{-1}

be observed by the short-term heat treatment with the maximum temperature of 200 °C. The same material behaviour is evident in the short-term heat treatments with higher maximum temperatures. During heating, the tensile and yield strengths decrease with increasing temperature, whereas the strengths increase again during cooling. The softening after the short-term heat treatment increases with the rising maximum temperature.

As can be seen in the example of the yield and tensile strength, the mechanical properties of the investigated alloy depend on the maximum temperature during the short-term heat treatment. This behaviour correlates with the findings from the thermal analysis. Up to the maximum temperature of 200 °C, the yield and tensile strength are only slightly reduced after the short-term heat treatment. The main softening takes place between temperatures of 200 and 300 °C. In this temperature range, the strength-increasing clusters and GP-zones of the initial state are dissolved [8]. Between temperatures of 300 °C and 400 °C, the yield and the tensile strengths are slightly reduced with rising temperature.

Furthermore, it was shown that the mechanical properties of the alloy EN AW6082 T4 during heating differ from those during cooling. They strongly depend on the heat treat-

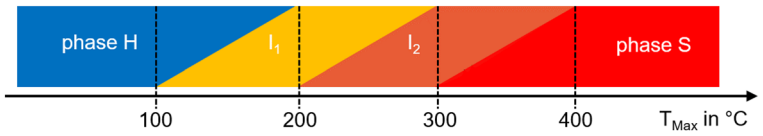

Fig. 5 Temperature transformation ranges of the imaginary phases for alloy EN AW6082 T4

ment history besides the current temperature. This mechanical behaviour of the alloy EN AW6082 T4 during the short-term heat treatment is to be modelled in the numerical simulation. For this purpose, a model approach for a low strength alloy 6060 [12] is further developed for the present high strength alloy 6082. For this purpose, the initial state is defined as an imaginary hardened phase (H), while the softened state after higher maximum temperatures is defined as an imaginary softened phase (S). These phases are transferred to each other depending on the temperature during heating. During cooling, no phase transformation is defined, because typical cooling rates of about 10 Ks^{-1} exceed the critical cooling rates of most 6XXX alloys [13]. The virtual phases are assigned to temperature-dependent flow curves. The material model does not consider the heating or cooling rate. Therefore, flow curves, which were recorded during a typical short-term heat treatment, i.e. during a rapid heating of about 100 Ks^1 and during a cooling rate of a few 10 Ks^1, have to be assigned to the virtual phases. A detailed description of the material model for the alloy EN AW6060 T4 can be found in reference [12].

Intermediate phases can be implemented between the imaginary hardened phase (H) and the imaginary softened phase (S), to describe the material behaviour more accurately. In order to be able to map the relatively large softening range of the alloy EN AW6082 T4, two intermediate phases (I_1 and I_2) were implemented. The transformation temperatures of the individual imaginary phases have been defined according to the continuous heating dissolution diagram [8]. Figure 5 shows the temperature transformation ranges of the imaginary phases for alloy EN AW6082 T4. The alloy is slightly softened by a short-term heat treatment up to the maximum temperature of 200 °C. This is considered in the material model by implementing the intermediate phase (I_1) at 200 °C. Most of the softening takes place in the peak temperature range between 200 °C and 300 °C. For this reason, at the maximum temperature of 300 °C, the intermediate phase (I_2) is inserted. The mechanical properties do not change further after the short-term heat treatment above the peak temperature of 400 °C. For this reason, it is defined that from the maximum temperature of 400 °C, only the softened imaginary phase (S) is present. The individual phases change linearly depending on temperature, as Fig. 5 shows schematically. In LSDyna the keyword ***MAT_GENERALIZED_PHASECHANGE** predefines different phase transformation laws. Only one of the predefined phase transformation laws can be linearised. This is the phase transformation law according to Johnson-Mehl-Avrami-Kolmogorov (JMAK) [14].

The temperature-dependent flow curves of the single imaginary phases have been described by the Hockett-Sherby function [15]. A detailed description of the calculation of the temperature-dependent flow curves and Hockett-Sherby parameters from the experimental data can be found in reference [12].

A simple geometric model was used to verify the mechanical material model of alloy EN AW6082 T4. The simulation model consisted of a single cube-shaped solid element with an edge length of 1 mm. This element was subjected to a defined temperature profile

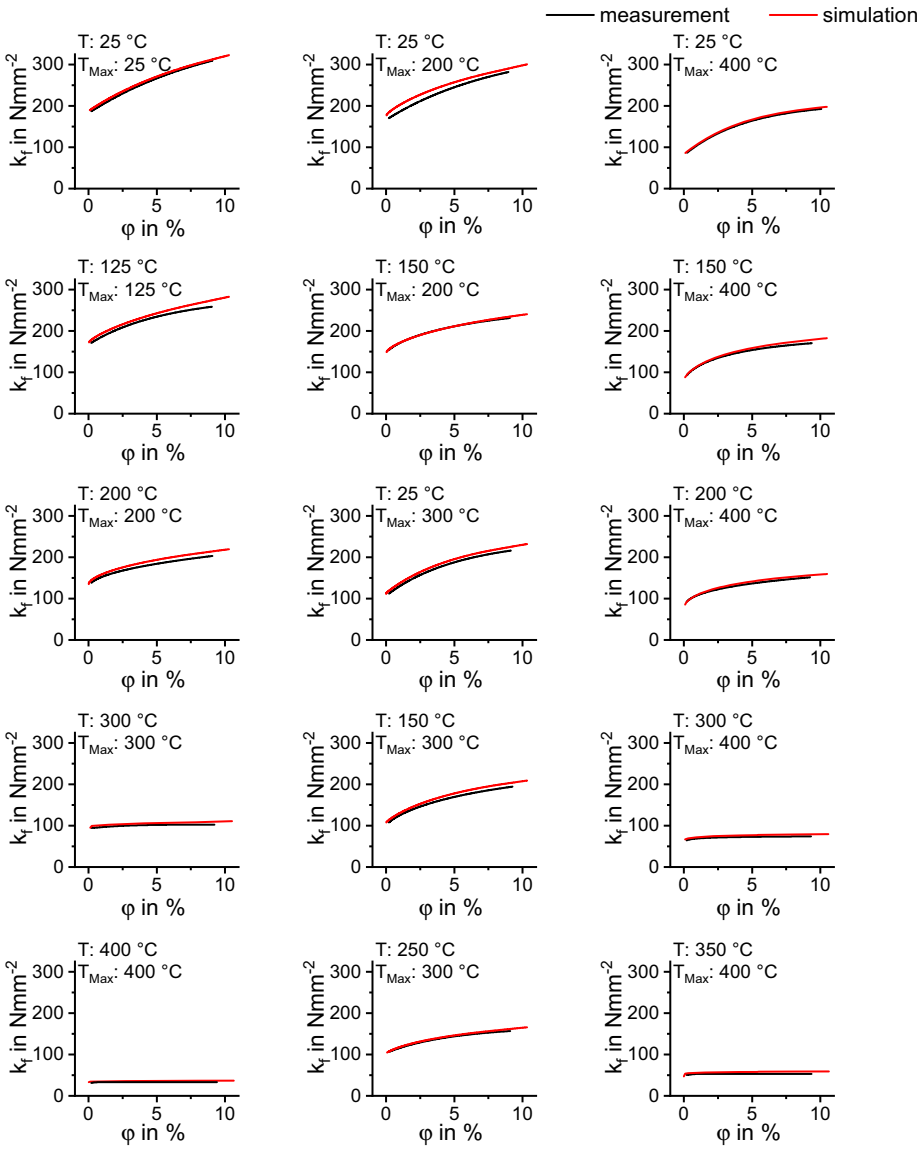

Fig. 6 Experimentally determined and simulated flow curves after different short-term heat treatments

to simulate heat treatment. The element was firmly clamped on one side by boundary conditions. The nodes on the other side were loaded with a predetermined displacement. Thermal expansion was not considered during this simulation to prevent thermally induced deformation. The time-temperature curve was varied in both the maximum temperature, and in the temperature during deformation, in different individual simulations. The time-displacement curve remained constant during all individual simulations. The simulated flow curves were then compared with experimental data. Figure 6 clearly shows that the material model adapted to EN AW-6082 T4 provides very good agreement between the experimental and simulated flow curves.

It has been demonstrated that the material model calculates the mechanical properties during a short-term heat treatment very well, while the most important factors, the maximum temperature, the temperature path, and the current temperature are considered.

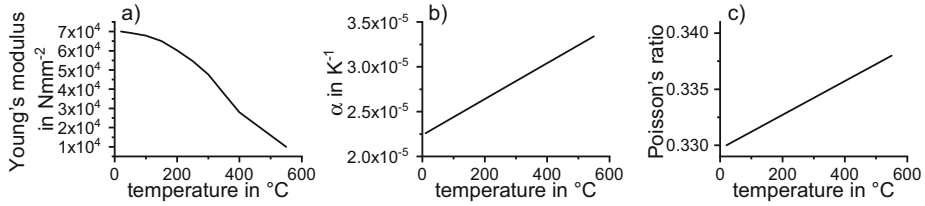

Fig. 7 Implemented temperature-dependent material properties; **A** Young's modulus; **B** coefficient of thermal expansion; **C** Poisson's ratio [16]

The material model can therefore be regarded as valid with regards to the mechanical properties. The material model is subsequently transferred to the laser heat treatment of the extrusion profile.

Heat treatment simulation model

The hollow extrusion profile with a cross section of 40 × 40 × 3 mm and a length of 330 mm was modelled in the FE-Software LS-Dyna by cubic solid elements with an edge length of 1 mm. The previously validated model for the alloy EN AW-6082 T4 was used as a mechanical material model. For the simulation, thermo-mechanical modelling is used, which is then solved using an explicit approach. The initial temperature is 25 °C. The boundary conditions were determined by a convective heat transfer at an ambient temperature of 25 °C, and a heat transfer coefficient of 2.5 $Wm^{-2}K^{-1}$. The heat input by laser was implemented in the simulation model by a moving heat source. Via the keyword ***BOUNDARY_FLUX_SET**. The time-varying power of the laser to reach the specified temperature was extracted from the experimental power control data and used as an input for the heat treatment simulation.

Further material parameters must be defined for the material model. The specific heat capacity was defined as 896 $Jkg^{-1}K^{-1}$, and the thermal conductivity as 180 $Wm^{1}K^{1}$. The material density was set at 2.7 g cm^{-3}. Young's modulus, coefficient of thermal expansion, and Poisson's ratio were defined as temperature-dependent, as shown in Fig. 7.

Validation of short-term heat treatment simulation

For the temperature validation, a laser short-term heat treatment was performed on a real aluminium extrusion profile by a diode laser (LDM3000-100, P_{Max}: 3 kW, λ: 940 nm). Due to the use of a zoom and homogeniser optic, a homogeneous intensity distribution can be assured over the rectangular spot, which was adjusted to 20 mm × 40 mm. For the heat treatment, the optic was moved by a robot system with a velocity of 10 mms^{-1}. During the heat treatment the material temperature was measured by means of a pyrometer, and adjusted by a power control to a predetermined value of 450 °C. In addition, the time dependent temperatures on the profile were recorded by an infrared camera.

For the validation of the laser heat treatment simulation, a layout needs to be used which resembles the later THTP. A heat treatment on the flanges of the profile can increase the maximum bending angle and decrease the cross-section deformations by direct and indirect influence of the appearing compressive and tensile stresses [17]. However, a certain distance between the heat treatment zone and the forming zone is mandatory to avoid extensive thinning in the softened zone and collapsing of the cross-section. The movement of the laser spot with a size of 40 mm × 20 mm was started 30 mm from

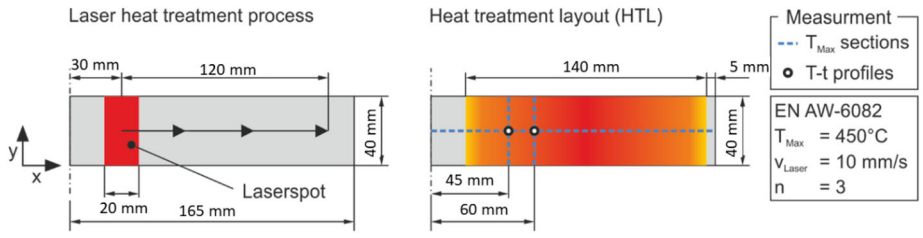

Fig. 8 Heat treatment layout and temperature measurement (half profile length)

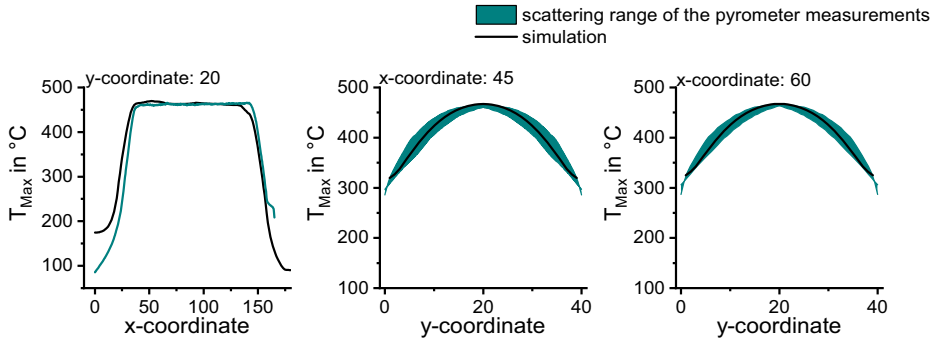

Fig. 9 Measured and simulated maximum temperature on the profile surface at different positions

the centre and stopped 15 mm from the end of the profile (Fig. 8). Thereby, an almost untreated length of 20 mm from the centre of the profile is created, followed by the softened heat treatment zone. In real heat treatments, this layout is carried out with the laser, starting in the middle of the profile and moving outwards in one X-direction, and then from the middle of the profile in the other X-direction. This is repeated on the other flange side of the profile. For the validation of the temperature distribution, we used the first laser track. The temperature during laser short-term heat treatment was determined on the profile axis and at two points (45 mm and 60 mm distance to the profile centre) perpendicular to the profile axis.

Figure 9 shows the measured and simulated maximum temperature on the profile surface at the different positions. Figure 9A shows that the simulated maximum temperature on the profile surface along the profile axis agrees very well with the measured values. Only at the beginning of the profile are slightly higher temperatures simulated. As can be seen from Fig. 9B and C, the simulated perpendicular temperature distribution is also in the scattering range of the pyrometer measurements during a real laser heat treatment.

Figure 10 shows the measured and simulated temperature-time curves at two different positions on the heat-treated profile. It becomes clear that the heating path is reproduced very well at both positions. During cooling there is a slight deviation in the temperature profile. However, the general course of the temperature is well mapped. It has been shown that the temperature distribution measured during a real laser short-term heat treatment agrees very well with the simulated temperature distribution. The simulation model can therefore be regarded as valid with regards to the temperature distribution.

Figure 11 shows the phase distribution of the four virtual phases after the heat treatment. The mechanical properties after the short-term heat treatment are derived from this phase distribution, and are adopted as input parameters in the forming simulation.

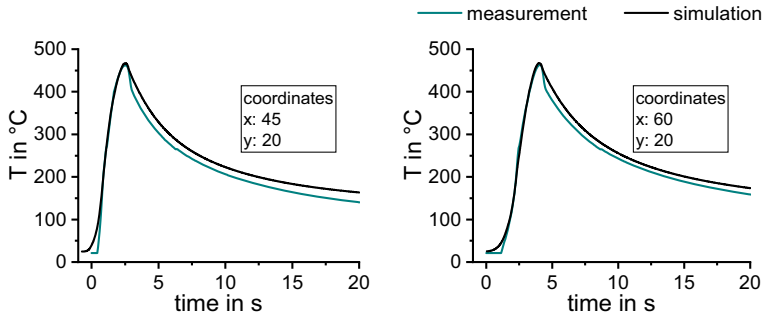

Fig. 10 Time temperature profile during laser short-term heat treatment at two different positions, measured and simulated

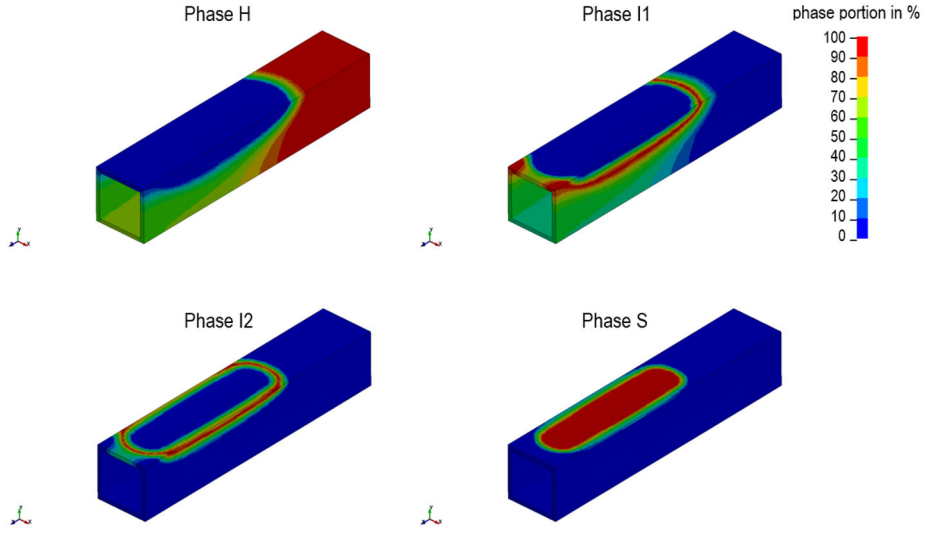

Fig. 11 Distribution of the virtual phases after the short-term heat treatment

Figure 12 shows the deformation of the heat-treated profile, 20 times enlarged, as well as exemplary the residual stresses in the z-direction after the short-term heat treatment.

Forming simulation—bending of hollow profile

An important basis for the bending simulation is the characterisation of the mechanical properties of the extrusion alloy EN AW-6082. Especially the anisotropic behaviour of the material under load in the extrusion direction (ED), diagonal direction (DD) and transverse to the extrusion direction (TD), needs to be identified after short-term heat treatments with various maximum temperatures. The identified yield strength and Lankford coefficient values are then used to design the yield locus curves (YLC) according to [18], and the flow curves are approximated and extrapolated with the Hockett-Sherby formula.

Characterisation of anisotropic material behaviour

Aluminium extrusion profiles exhibit high anisotropic behaviour. Thus, load direction dependent material parameters have to be characterised by uniaxial tensile tests in the ED, DD and TD. However, due to the small geometrical dimensions of the semi-finished

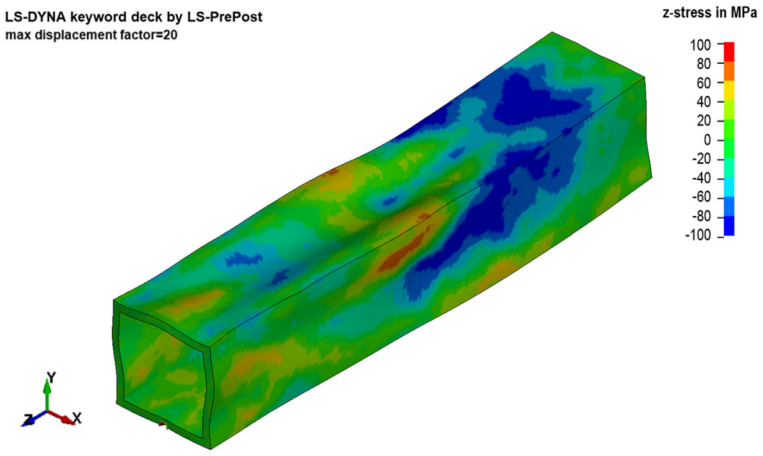

Fig. 12 Deformation of the heat-treated profile, 20 times enlarged, as well as the residual stresses in the z-direction after the short-term heat treatment

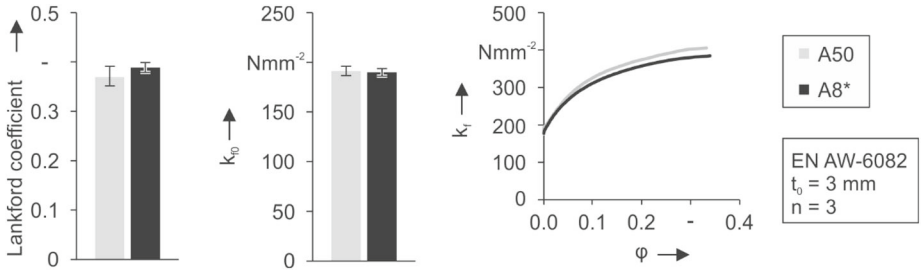

Fig. 13 Comparison of conventional specimen A50 and miniaturised specimen A8*

products, which in case of the investigated aluminium profiles are only 40 mm in height and width, conventional tensile specimens with a length of 150 mm can only be produced in the ED. Due to this fact, the design of a new specimen geometry with reduced dimensions is needed, considering material, manufacturing, and testing aspects. The identified specimen has a thickness of 3 mm, a measuring width of 6 mm and a measuring length of 8 mm (designated as A8*). The characterisation results of the miniaturised and the conventional specimens were compared regarding the flow curve, as well as the Lankford coefficient and yield strength in the ED in Fig. 13.

Regarding the identified Lankford coefficient, the value for the miniaturised specimen is slightly higher, but still in the range of the standard deviation. The accordance between both yield strengths is even better. However, with regard to the flow curves, the miniaturised specimens show slightly lower strain hardening than conventional specimens. For the purpose of analysing the influence of the short-term heat treatment on the anisotropic behaviour, miniaturised specimens were laser heat treated with a heating rate of 100 Ks^{-1}, a soaking time of 0.1 s in a temperature range from 200 °C to 450 °C in 50 °C steps, and a cooling rate of approximately 5 Ks^{-1}.

The identified Lankford coefficients show only a small dependence regarding the applied maximum heat treatment temperature T_{Max} (Fig. 14). However, high differences between the different load directions exist. In the ED, the Lankford coefficient increases from 0.41±0.01 to 0.52±0.01 in the temperature range of 200 °C to 400 °C. In contrast, the values in the DD decrease in the same temperature range from 1.90±0.01 to 1.78±0.04.

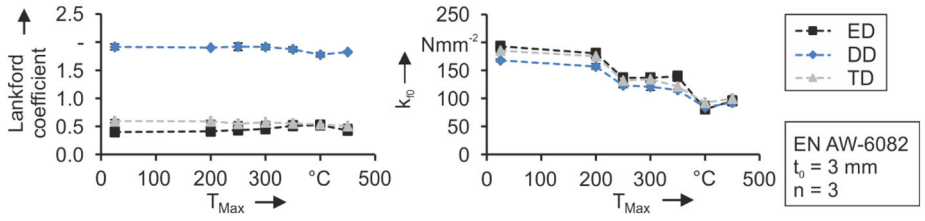

Fig. 14 Results of tensile test characterisation with miniaturised specimens

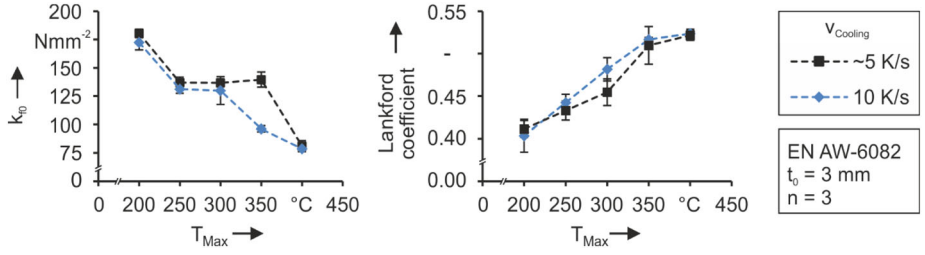

Fig. 15 Comparison between different cooling velocities under load in ED

Also, in the TD, a decrease of the Lankford coefficient from 0.59±0.02 to 0.53±0.01 can be identified. Thus, the material under load in the DD preferably flows out of the material plane, whereas in the ED and TD, it mainly flows out of the material thickness, leading to earlier strain localisation and necking failure. In addition, the yield strength also shows load direction dependent behaviour. For the initial state T4, the lowest yield strength appears in the DD with 168 Nmm^{-2}. In the TD a value of 186 Nmm^{-2} and in the ED, the highest yield strength with 193 Nmm^{-2} was identified. The ratio between the different load directions nearly persists until the maximum heat treatment temperature of 350 °C. For higher heat treatment temperatures, no significant difference can be detected. Similar to the results from the thermomechanical analysis (Fig. 4), softening of the material starts at 200 °C. However, the yield strength is slightly higher for the laser heat treated miniaturised tensile specimens. This is mainly due to natural ageing during the transfer time of 1 h between the heat treatment and tension test, as well as the slower cooling rate of 5 Ks^{-1} instead of 10 Ks^{-1}. Therefore, further experiments with a higher cooling rate of 10 Ks^{1} were conducted.

Due to the higher cooling rate a slight overall decrease of the yield strength in comparison to the lower cooling rate, as well as a significant higher softening in the temperature range of 250 °C to 350 °C was achieved (Fig. 15). Because no significant influence of the cooling rate on the Lankford coefficients was identified, the Lankford coefficients for the three load directions were taken from the results of 5 Ks^{-1}.

Modelling of the anisotropic material behaviour

For modelling of the anisotropic material behaviour, an extrapolation of the flow curves to higher strain values, as well as a yield locus model have to be used.

Flow curves

Similar to the above thermo-mechanical model, the formula according to Hockett-Sherby was used for the extrapolation of the flow curves for the T4 state i.e. 25 °C, 200 °C, 300 °C and 400 °C, which resemble the respective phases H, I1, I2 and S (Fig. 16).

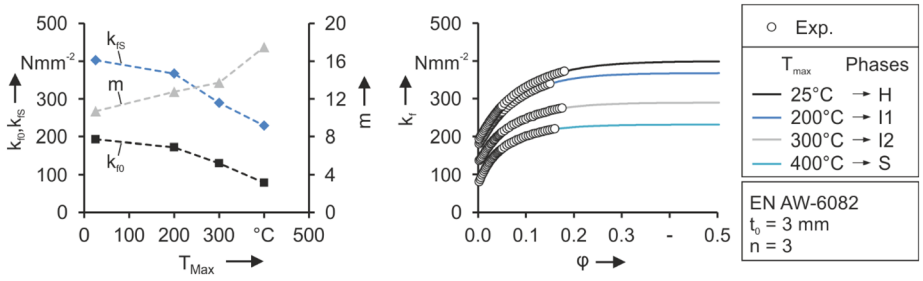

Fig. 16 Identified Hockett-Sherby parameters and respective flow curves in ED

T_{Max} in °C	$k_{f0,ED}$ in Nmm^{-2}	LC_{ED}	LC_{DD}	LC_{TD}
25	192.8	0.398	1.916	0.592
200	172.4	0.411	1.902	0.586
300	129.9	0.455	1.914	0.569
400	78.7	0.522	1.777	0.541

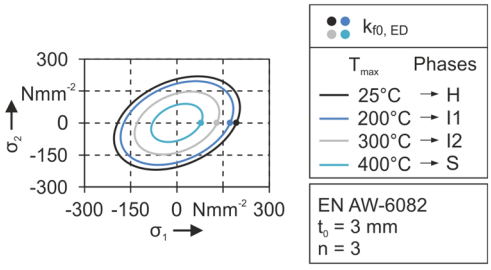

Fig. 17 Mechanical properties and identified YLCs according to Hill model

The parameter k_{f0} was chosen according to the respective start of yielding identified in the uniaxial tensile tests. k_{fs} decreases with increasing heat treatment temperature T_{Max}, which fits the real softening of the material due to the short-term heat treatment. Parameter m in combination with parameter P describe the strain hardening of the material. For simplification purposes, parameter P was set to a constant value of 1.0, because a sufficient description of the strain hardening of the material can be achieved by a sole variation of parameter m. From T_{Max} = 25 °C to 400 °C, parameter m rises from 10.7 to 17.5, which indicates an increase of the hardening coefficient. For a complete description of the material behaviour besides the flow curves, the start of yielding in dependence of the stress state defined by the so-called yield locus curve (YLC) is mandatory.

Yield locus curves

For the depiction of the stress state dependent yielding of the aluminium extrusion alloy EN AW-6082, the yield locus model of [18] was chosen and implemented in the keyword **`*MAT_ANISOTROPIC_VISCOPLASTIC`** in LS-Dyna. The model uses the yield strength in the extrusion direction, as well as the Lankford coefficients in the ED, DD and TD. With these four values the four needed Hill parameters F, G, H and N can be directly calculated. The other two parameters L and M are set to the standard value of 1.5.

Because of the small deviations of the Lankford coefficients (LC) for the four temperatures, only small differences regarding the geometry of the yield locus curves are present (Fig. 17). Thus, for simplification purposes, an averaged value for the Lankford coefficients also seems practicable, which would result in one shape of the yield locus curve solely scaled by the temperature dependent yield strength. However, in this case, the individually identified LC values are used for each heat treatment temperature.

Modelling of the bending process

The bending process, in this case, is a three-point bending test (Fig. 18a). The profile with a length of 330 mm is placed on two supports with radii of 25 mm and a contact

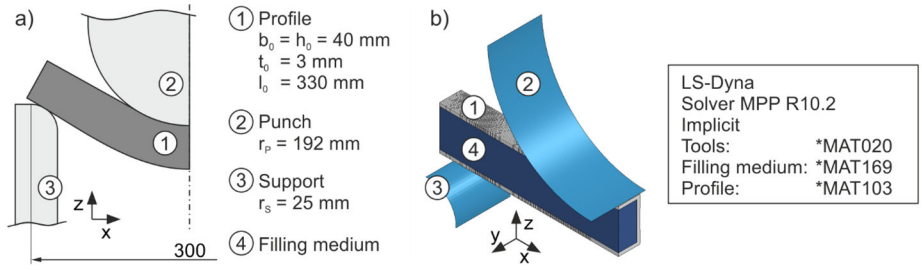

Fig. 18 Three-point bending test rig and simulation model

point distance of 300 mm. The centred punch with a radius of 192 mm is moved with a velocity 1 mms^{-1} for 60 mm, whereby the profile is bent. For the purpose of reducing cross-section deformations, the profile is filled with a ceramic granulate and sealed before the bending process. After the punch has reached 60 mm, it moves back to its starting position and the elastic strains in the profile are released, which leads to springback. For the validation of the bending simulation, a deterministic point pattern is applied to the surface of the profile before bending. By optical measurement of the deformed pattern with a GOM Argus system, the locally appearing strains can be identified and compared to the numerical results.

In bending simulation similar to most sheet metal forming simulations, only the contact areas of the tools are modelled with shell elements and rigid behaviour using ***MAT020_RIGID**, which means the elastic deformation of the tools is neglected. Similar to the experimental test, the support is static and the punch is moving. The ceramic granulate which is used as filling medium, is depicted by ***MAT169**, which is specifically used to imitate the material behaviour of sands and soils [19]. The material parameters used in the model are defined according to former characterisation test conducted by [20]. The extrusion profile itself is modelled with volume elements with an edge length of 0.5 mm, which corresponds to six elements across the thickness of the extrusion profile in order to be able to precisely depict the stress and strain state differences across the material thickness as well as the resulting material flow during the bending process [21]. As contact formulation between the profile, the filling medium and the tools ***CONTACT_AUTOMATIC_SINGLE_SURFACE_MORTAR** is used, which provides fast calculation of the contact forces and good convergence in implicit simulations. In addition, by using the implicit calculation approach, the achievement of equilibrium during the bending process and after the springback of the profile is assured [22]. After the simulation of bending and springback, the quarter model can be mirrored into a full representation of the profile, with the resulting stresses and strains and therefore is utilizable for validation with experimental tests.

Linked heat treatment and bending simulation

Data transfer between heat treatment and bending simulation

Because up to now there is no suitable material model in LS-Dyna which allows for the phase dependent anisotropic behaviour for volume elements, a subroutine is needed for data transfer between the heat treatment and bending simulation. Therefore, the programming language Matlab was used. The subroutine is divided into three steps: Output analysis, parameter calculation, and input generation.

Output analysis of the heat treatment simulation

The FE-result of the profile after laser heat treatment simulation is exported with all data consisting of residual stresses and strains, as well as the percentage phase mixture for every volume element which was used to model the extrusion profile. This data is imported in Matlab and elements with the same phase mixture of H, I1, I2 and S are assigned to one material state. In the case of the investigated profile, 532 material states with different phase mixtures were identified.

Parameter calculation

Each of the four phases is related to one flow and one yield locus curves (Fig. 16), which are weighted according to the phase mixtures, resulting in a set of 532 flow and yield locus curves. The calculated parameters for the yield locus model according to Hill are inserted in keyword **`*MAT_ANISOTROPIC_VISCOPLASTIC.`** For the flow curves, stress–strain data is written to curve files (**`*DEFINE_CURVE`**) which are referred to in the material keyword. The FE-model of the extrusion profile is partitioned into 532 subparts, wherefore they can be referenced to the different calculated material properties. This allows to create a FE-model of the extrusion profile with different elasto-plastic and anisotropic behaviour according to the state after the local short-term heat treatment.

Input generation for bending simulation

Finally, the node and element data from the output file (residual stresses, strains and displacements resulting from the laser heat treatment) is added to the FE model of the extrusion profile and a new input file for LS-Dyna is generated and the subroutine is finished. For further improvement of the simulation quality, the edge length of the profile mesh is halved from 1 mm (heat treatment simulation) to 0.5 mm (bending simulation) to get a better depiction of the stresses and strains which appear during bending of the profile. The input file with all results, geometric data, and material parameters, is imported into the bending simulation.

For validation, the hardness distribution of the profile after the application of the heat treatment layout on the flanges of the profile is compared to the calculated yield strength, which is elementwise assigned to the profile after the usage of the subroutine. The hardness is measured in the centre of the profile and at 3 mm distance to each other in the area from 14 mm to 26 mm from the centre (Fig. 19). The hardness in the centre of the profile is about 82 HV5. From 14 mm to 20 mm no significant reduction of the hardness is identified. At 23 mm, the hardness decreases to 72 HV5 and further to 62 HV5 at 26 mm. The yield strength in comparison decreases from 192 Nmm^{-2} in the centre to roughly 178 Nmm^{-2} at 20 mm. After 20 mm, the yield strength decreases significantly to 156 Nmm^{-2} at 26 mm. The hardness and yield strength distribution correlate with each other, similar to the hardness/tensile strength relation suggested by [23].

Validation of the process chain by numerical and experimental bending results

For the final validation of the numerical process chain, the results of the experimental bending tests are compared to the numerical results of the bending simulation. Strains appearing on the critical outer radius of the profile were identified by optical strain measurement as already described. In this context, it has to be mentioned that the strains on the edges of the profile were hard to evaluate and therefore excluded from the analysis and depiction in Fig. 20. The comparison between numerical and experimental data shows

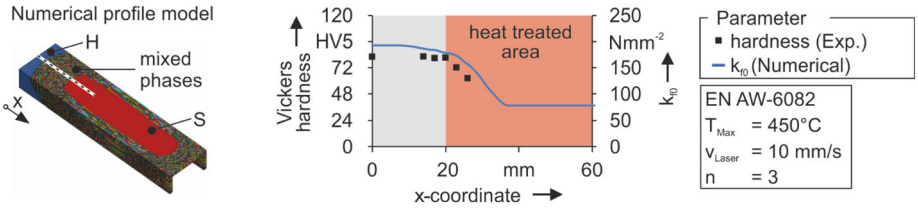

Fig. 19 Hardness comparison to calculated yield stress in ED

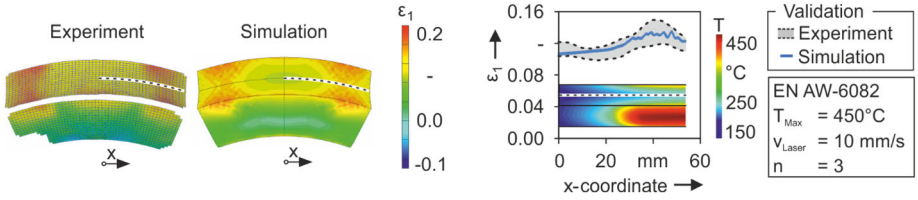

Fig. 20 Comparison of strains appearing on the outer radius of the profile

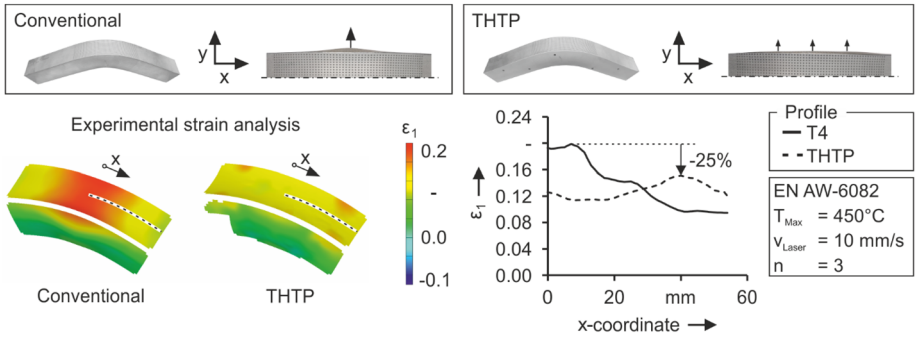

Fig. 21 Cross-section deformations and experimental optical strain measurement results for a conventional profile and the local short-term heat treated THTP

good accordance (Fig. 20). The numerical strain in the centre of the profile of roughly 0.11 agrees with the minimum value of the experimental scatter band. Furthermore, the simulation shows good agreement regarding the increase of the maximum principal strain, up to approximately 0.13, in the area around 30 to 50 mm due to the improved material flow in the softened zone.

Improvement of bendability by THTP

The improvement of bendability by the chosen heat treatment layout is identified by optical strain measurements (Fig. 21). For the initial EN AW6082 T4 profile, a maximum principal strain of roughly 0.2 was identified in the centre of the profile, which gradually decreases to 0.09 at x = 55 mm. Due to THTP on the flanges of the profile, the material flow from the softened areas into the critical forming zone is improved and process forces are reduced, leading to a reduction of the appeared strains. In the centre of the profile, the maximum principal strain decreases by about 35% to 0.13. In addition, the material flow adjacent to the heat-treated zones of the flanges is improved on the outer radius, whereby the strains in the area of 30 mm to 55 mm to the centre rise. The result is a more homogeneous strain distribution, with a reduction of the maximum strain value of roughly 25% in comparison to the initial profile. As a consequence of the better strain

distribution, cross-section deformations concentrated in the forming zone are reduced as well.

Conclusion

The application of Tailor Heat Treated Profiles (THTP), i.e. local heat treatment layouts, is feasible to enhance the forming limits of aluminium extrusion profiles in bending processes. However, precise numerical calculations are mandatory to design purposeful heat treatment layouts. In this investigation, a numerical process chain model was presented, combining a thermo-mechanical laser heat treatment simulation with a mechanical tube bending simulation. In addition, all fundamental experimental investigations are shown, which are needed to describe the change of material properties during and after short-term heat treatment. The following findings have been made:

- For the numerical simulation of the laser short-term heat treatment, a material model was developed for the investigated alloy EN AW6082 T4. It is able, to describe the flow curves depending on the maximum temperature, the temperature path, and the current temperature during a short-term heat treatment.
- This material model was implemented in a laser heat treatment simulation of an extrusion profile. As a result of the thermomechanical simulation, the resulting local flow curves, as well as the resulting residual stresses and distortions, can be calculated after the heat treatment.
- By targeted linking of the thermomechanical heat treatment simulation with the subsequent forming simulation, considering anisotropic material behaviour, a continuous process chain simulation for the production of THTP was developed. The validation of the different simulation steps was successfully carried out by systematically comparing simulations and experiments. The heat treatment layout for the production of THTP and the heat treatment parameters required for this can be optimised by means of numerical simulation.
- The linked model can be adapted to other alloys and geometries. Component tests during the design of THT processes for new alloys and geometries can thus be significantly reduced, and costs can be saved.
- In order to expand the field of application for the material model and thus the linked heat treatment simulation, a dependency of the cooling rate should be implemented in the material model. This means that short-term heat treatments can also be simulated on more massive components.

Acknowledgements

The authors would like to thank the German Research Foundation (DFG) for supporting the present investigations within the scope the research project "Improvement of formability of extruded aluminium profiles by a local short-term heat treatment (DFG KE616/22-2 / DFG ME2043/45-2)".

Author contributions

HF: Conceptualization, methodology, data curation, investigation, writing—original draft, Writing—review and editing. MG: Conceptualization, methodology, data curation, investigation, writing—review and editing. MR: Methodology, data curation, investigation, writing—review and editing. ML: Methodology, investigation, writing—review and editing. MM: Conceptualization, resources, project administration, writing—review and editing, supervision. OK: Conceptualization, resources, project administration, writing—review and editing, supervision. All authors read and approved the final manuscript.

Funding

Open Access funding enabled and organized by Projekt DEAL. This work was funded by the German Research Foundation (DFG) through the research project "Improvement of formability of extruded aluminium profiles by a local

short-term heat treatment (DFG KE616/22-2 / DFG ME2043/45-2)". Open Access funding enabled and organized by project DEAL. We acknowledge funding by German Research Foundation and University of Rostock – 512855535.

Availability of data and materials
The datasets used and analysed during the current study are available from the corresponding author on reasonable request.

Declarations

Competing interests
The authors declare that they have no competing interests.

Received: 9 January 2023 Accepted: 24 May 2023
Published online: 12 June 2023

References

1. Polmear IJ. Light alloys: from traditional alloys to nanocrystals. 4th ed. Amsterdam: Elsevier Butterworth-Heinemann; 2006.
2. Geiger M, Merklein M, Vogt U. Aluminum tailored heat treated blanks. Prod Eng Res Devel. 2009;3:401–10. https://doi.org/10.1007/s11740-009-0179-8.
3. Vollertsen F, Lange K. Enhancement of drawability by local heat treatment. CIRP Ann Manuf Technol. 1998;47:181–4. https://doi.org/10.1016/S0007-8506(07)62813-3.
4. Geiger M, Merklein M, Staud D, Kaupper M. An inverse approach to the numerical design of the process sequence of tailored heat treated blanks. Prod Eng Res Devel. 2008;2:15–20. https://doi.org/10.1007/s11740-007-0072-2.
5. Kahrimanidis A, Lechner M, Degner J, Wortberg D, Merklein M. Process design of aluminum tailor heat treated blanks. Mater. 2015;8:8524–38. https://doi.org/10.3390/ma8125476.
6. Fjeldly A, Roven HJ. Observations and calculations on mechanical anisotropy and plastic flow of an AlZnMg extrusion. Acta Mater. 1996;44:3497–504. https://doi.org/10.1016/1359-6454(96)00015-8.
7. Paulsen F, Welo T. Application of numerical simulation in the bending of aluminium-alloy profiles. J Mater Process Technol. 1996;58:274–85. https://doi.org/10.1016/0924-0136(95)02152-3.
8. Fröck H, Reich M, Milkereit B, Kessler O. Scanning rate extension of conventional DSCs through indirect measurements. Mater. 2019. https://doi.org/10.3390/ma12071085.
9. Osten J, Söllig P, Reich M, Kalich J, Füssel U, Kessler O. Softening of high-strength steel for laser assisted clinching. Adv Mater Res. 2014;966–967:617–27. https://doi.org/10.4028/www.scientific.net/AMR.966-967.617.
10. Graser M, Fröck H, Lechner M, Reich M, Kessler O, Merklein M. Influence of short-term heat treatment on the microstructure and mechanical properties of EN AW-6060 T4 extrusion profiles–Part B. Prod Eng Res Devel. 2016;10:391–8. https://doi.org/10.1007/s11740-016-0684-5.
11. Fröck H, Graser M, Reich M, Lechner M, Merklein M, Kessler O. Influence of short-term heat treatment on the microstructure and mechanical properties of EN AW-6060 T4 extrusion profiles: Part A. Prod Eng Res Devel. 2016;10:383–9. https://doi.org/10.1007/s11740-016-0683-6.
12. Fröck H, Kappis LV, Reich M, Kessler O. A phenomenological mechanical material model for precipitation hardening aluminium alloys. Metals. 2019;9:1165. https://doi.org/10.3390/met9111165.
13. Milkereit B. Kontinuierliche Zeit-Temperatur-Ausscheidungs-Diagramme von Al-Mg-Si-Legierungen [Dissertation]. Rostock, PhD-Thesis, University of Rostock, Shaker Verlag, Aachen, DOI: https://doi.org/10.2370/9783832299934:University of Rostock; 01.03.2011.
14. Johnson WA, Mehl RF. Reaction kinetics in processes of nucleation and growth. Trans Am Inst Mining Metall Petrol Eng. 1939;135:416–42.
15. Hockett JE, Sherby OD. Large strain deformation of polycrystalline metals at low homologous temperatures. J Mech Phys Solids. 1975;23:87–98. https://doi.org/10.1016/0022-5096(75)90018-6.
16. Kammer C, editor. Aluminium-Taschenbuch. 17th ed. Berlin: Beuth; 2014.
17. Graser M, Pflaum N, Merklein M. Influence of a local laser heat treatment on the bending properties of aluminium extrusion profiles. Procedia CIRP. 2018;74:780–4. https://doi.org/10.1016/j.procir.2018.08.011.
18. Hill R. A theory of the yielding and plastic flow of anisotropic metals. Proc Roy Soc London. 1948;1948:281–97.
19. Drucker DC, Prager W. Soil mechanics and plastic analysis or limit design. Quart Appl Math. 1952;10:157–65. https://doi.org/10.1090/qam/48291.
20. Grüner M, Merklein M, Franke J. Schmidt. Hochdruck-Blechumformung mit formlos festen Stoffen als Wirkmedium: Meisenbach; 2014.
21. Tobias E. Review of solid element formulations in LS-Dyna—properties, limits, advantages, disadvantages. Switzerland; 12.10.2011.
22. Banabic D. Sheet metal forming processes: constitutive modelling and numerical simulation. Berlin, Heidelberg: Springer; 2010.
23. Ostermann F. Anwendungstechnologie Aluminium. 3rd ed. Berlin, Heidelberg: Springer-Verlag; 2014.

Publisher's Note